Bull. Mater. Sci.
DOI 10.1007/s12034-017-1487-9

Structural and optical properties of diluted magnetic $Ga_{1-x}Mn_xAs$–AlAs quantum wells grown on high-index GaAs planes

MUSTAFA GUNES[1,*], CEBRAIL GUMUS[2], YARA GALVÃO GOBATO[3] and MOHAMED HENINI[4]
[1]Department of Materials Engineering, Engineering and Natural Sciences Faculty, Adana Science and Technology University, 01250 Adana, Turkey
[2]Physics Department, Cukurova University, 01330 Adana, Turkey
[3]Departamento de Física, Universidade Federal de São Carlos, São Carlos, SP 13560-905, Brazil
[4]School of Physics and Astronomy, Nottingham Nanotechnology and Nanoscience Center, University of Nottingham, Nottingham NG7 2RD, UK
*Author for correspondence (mgunes@adanabtu.edu.tr)

MS received 24 May 2016; accepted 13 March 2017

Abstract. We report on the structural and optical properties of $Ga_{1-x}Mn_xAs$–AlAs quantum wells (QWs) with $x = 0.1\%$ grown by molecular beam epitaxy (MBE) on semi-insulating GaAs substrates with orientations (100), (110), (311)B and (411)B. Atomic force microscopy (AFM), X-ray diffraction (XRD) and photoluminescence (PL) techniques were used to investigate these QWs. AFM results have evidenced the formation of Mn-induced islands, which are randomly distributed on the surface. These islands tend to segregate for samples grown on (110) and (411)B planes, while no clear segregation was observed for samples grown on (100) and (311)B orientations. Results show that the PL line width increases with Mn segregation. XRD measurements were used to determine 2θ, d and cell parameters.

Keywords. AFM; MBE; photoluminescence; XRD; quantum well; GaMnAs.

1. Introduction

Diluted magnetic GaMnAs semiconductors have been considered as promising materials for applications in spin-based electronics, spintronics, ferromagnetic, microelectronic and optoelectronic devices [1,2].

Recently, the demonstration of large tunneling magnetoresistance induced by resonant tunneling in GaMnAs-based heterostructures made such structures to be in spin-dependent resonant tunneling diodes [3]. Experimental techniques such as magnetization, magneto-transport and ferromagnetic resonance measurements were used to explain magnetic properties of GaMnAs structures grown on different substrate planes. It was reported that the Hall resistance exhibited asymmetry with respect to magnetic field in GaMnAs structures grown in various orientations. It was explained that magnetization (M) is confined to preferred crystal planes, which could provide magnetic anisotropy in spintronic devices [4].

The achievement of high Curie temperature ($T_c = 110$ K) has accelerated the research on this material system, however, there are still growth challenges to obtain high-quality epitaxial layers which are required for these applications [5]. Some of the growth difficulties include the larger size and low vapour pressure of Mn as compared with Ga and As and low solubility of Mn in GaAs, and therefore low substrate growth temperature is required to grow high-quality GaMnAs [6]. However, generation of defects, such as As antisites and Mn interstitials, cannot be neglected as they can deteriorate the crystallinity of the material [7,8].

The incorporation of Mn in III–V semiconductors can be substitutional (occupies Ga or As sites) [9,10] and/or interstitial [11]. When Mn atoms occupy Ga sites, they act as acceptors (provide hole charges) and create natural magnetic moments [12]. For spintronic applications, high structural and electronic qualities are of paramount importance as well as high Curie temperature [13]. Spintronic devices, which are composed of multilayer heterostructures, are especially susceptible to the quality of the interfaces [14].

In this study, structural properties of $Ga_{0.999}Mn_{0.001}As$–AlAs quantum wells (QWs) grown by molecular beam epitaxy (MBE) on GaAs substrate in various orientations at relatively higher temperatures (450°C) are determined. The Mn content is kept low in order to avoid high density of defects. In fact, it was reported that for this low Mn composition the As defects are reduced and the substitutional incorporation of Mn into Ga sites is enhanced, which enabled the observation of optical emission [15]. The crystal quality of our QWs was determined by X-ray diffraction (XRD) measurements. The morphology and the surface roughness of the $Ga_{0.999}Mn_{0.001}As$–AlAs ternary alloys were determined by atomic force microscopy (AFM) technique. In addition, AFM

Published online: 31 October 2017

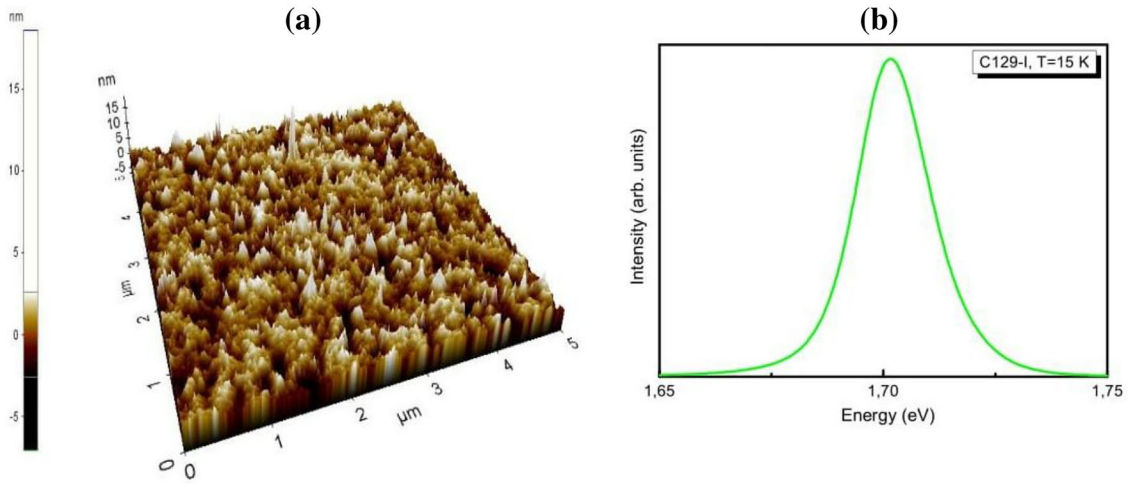

Figure 1. **(a)** AFM image of GaMnAs–AlAs QW grown on (100) plane and **(b)** PL spectrum of the same structure.

and XRD results are further supported by photoluminescence (PL) measurements.

2. Experimental

The samples were grown on (100), (110), (311)B and (411)B semi-insulating GaAs substrate planes in a Veeco Modular Gen II MBE reactor equipped with a real-time wafer temperature sensor, which allows accurate monitoring of the substrate temperature during growth. The structures were grown using As_4 species on In-free sample holders and consist of a GaAs buffer layer and an AlAs−GaAs−$Ga_{0.999}Mn_{0.001}As$ QW. During the GaMnAs QW growth, the As_4/(Ga+Mn) ratio was kept close to 1. The QW was surrounded by 50-nm thick AlAs barriers. The total QW thickness is 6 nm, which comprises two 1 nm layers of GaAs adjacent to the AlAs interfaces and a 4-nm thick GaMnAs layer. The structures were capped with a 10-nm GaAs layer. This configuration was used with the intent to reduce the effect of interface segregation of Mn, which might degrade the optical properties of the QW. The GaAs buffer layer and the rest of the structure were grown at 450°C. Structural properties were determined by Park System AFM and Rigaku smart Lab XRD, while PL measurements were performed using a Bruker VERTEX 80V Fourier transform infrared spectrometer equipped with PL module. A 532-nm continuous wave laser was used as an excitation source together with a Si-avalanche photodiode detector. All the PL measurements were taken at a temperature of 15 K. The samples are coded as C129-I, C129-II, C129-III and C129-IV for Mn-containing AlAs–GaMnAs QW structure grown on (100), (110), (311)B and (411)B GaAs substrates, respectively.

3. Results and discussion

Structural properties of GaMnAs QWs grown at higher temperatures and on different plane orientations were investigated by AFM and XRD techniques. The effect of the incorporation of Mn in GaMnAs QWs was studied and probed by PL measurements. Figures 1–4 show AFM and PL results for these GaMnAs QWs. It is well known that there is a tendency of Mn atoms to segregate to the surface, and this could be explained by the larger size and low vapour pressure of Mn as compared with Ga and As species. The segregation may occur during GaMnAs growth as seen in figures 2a and 4a. Hernandez *et al* [16] reported that uniform distribution of Mn into GaAs or GaMnAs multilayers with various Mn contents strongly depends on V–III flux ratio and substrate temperature. In the report, secondary ion mass spectrometry (SIMS) depth profile showed that Mn concentration near the sample surface is decreased from 7.2×10^{20} to 5.8×10^{20} atoms cm^{-3} at growth temperature $T = 250$ and 350 K, respectively [16]. It was concluded that the reduction in Mn concentration near the surface with increasing growth temperature is due to the absence of manganese segregation on the surface. Their results were further supported by AFM. No segregation was reported in the sample grown at $T = 350$ K. It was suggested that manganese distribution into GaAs along the growth direction is strongly dependent on the growth temperature [16]. Poggio *et al* [17] reported Mn concentration profile of GaMnAs–AlGaAs QW structure with various Mn contents using SIMS. The highest manganese concentration measured was in the range of $10^{18}-10^{20}$ atoms cm^{-3} at the centre of QW and decreased towards the sample surface down to $10^{17}-10^{19}$ atoms cm^{-3}. The Mn content on the sample surface, which is 100 nm above the QW region, was attributed to residual Mn concentration incorporated into the structure even if Mn shutter was shut during the surface epilayer growth. Furthermore, the presence of Mn impurities in the investigated samples was substitutionally incorporated [17]. In our investigation, Mn content (0.1%) and growth temperature (450°C) were kept constant while the GaAs substrate orientation was varied. Our AFM results have shown that there is no Mn segregation on the surface and the surface is nearly homogenous for (100)

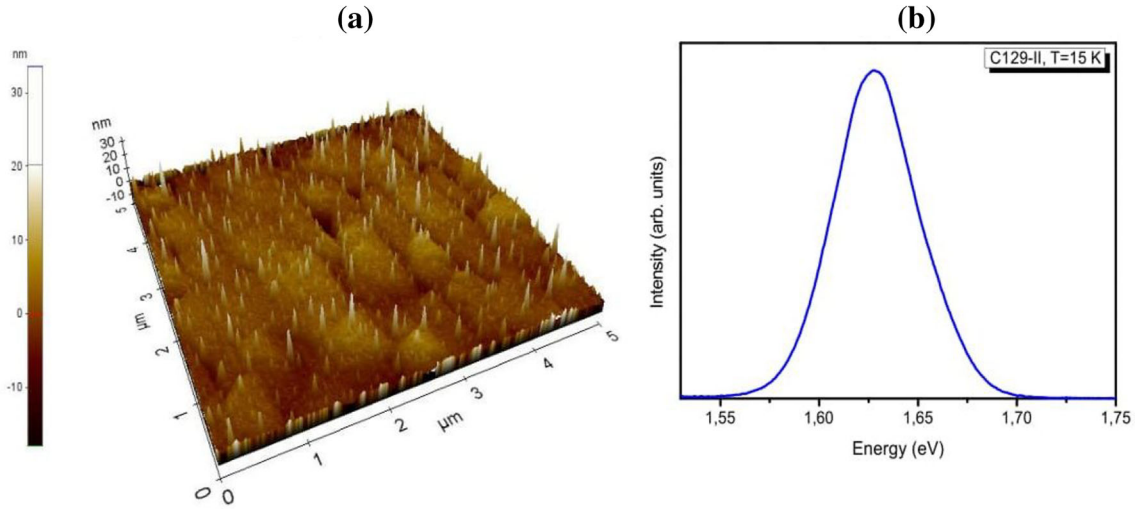

Figure 2. (a) AFM image of GaMnAs–AlAs QW grown on (110) plane and **(b)** PL spectrum of the same structure.

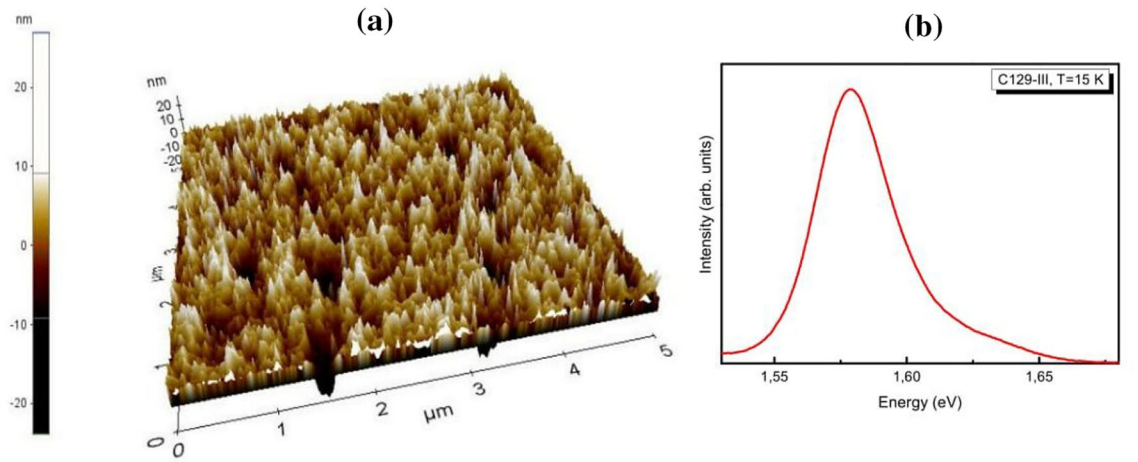

Figure 3. (a) AFM image of GaMnAs–AlAs QW grown on (311)B plane and **(b)** PL spectrum of the same structure.

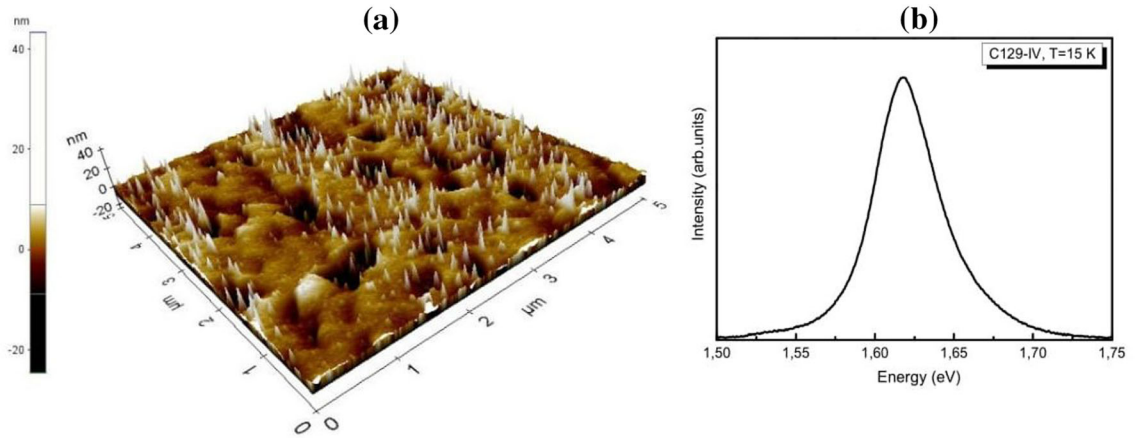

Figure 4. **(a)** AFM image of GaMnAs–AlAs QW grown on (411)B plane and **(b)** PL spectrum of the same structure.

plane while there is Mn segregation on the (110) surface. At high-index planes such as (311)B, Mn segregation on the surface was not observed. However, for (411)B plane the Mn segregation on the surface as determined by AFM is very high. This might be attributed to residual concentration of Mn (residual impurity), which incorporates into the structure even after the Mn shutter is closed, inducing non-homogenous surface. Gunes *et al* [15] and Rodrigues *et al* [18] recently reported PL results of (100) GaAs–AlAs QW structure with and without Mn content. The temperature-dependent PL spectrum in Mn-free GaAs–AlAs QW sample had a shallow donor, which was assigned to interstitial Mn_i. As a result, strong surface Mn segregation might be explained in terms of high residual Mn contamination during the growth. The differences in morphology, symmetry and surface reconstruction between the crystalline orientations of the substrate may be responsible for the dissimilar Mn segregations in the conventional (100) and non-(100) GaAs surfaces.

Manganese segregation on the surface of (411)B sample showed anomalous behaviour, having different concentrations at different parts of sample surface (see figure 4a). This might be attributed to Mn-rich and lower segregation. Furthermore, XRD measurements also confirmed the structural disorder, resulting in low crystal quality as seen in figure 5.

The surface roughness as measured by AFM is 5, 34, 16 and 38 nm for (100), (110), (311)B and (411)B, respectively (see figures 1a–4a). The magnitude of the roughness is related to the manganese segregation on the surface. Since no segregation is observed in (100) and (311)B, the surface roughness is very low, while in (110) and (411)B orientations the magnitude of surface roughness is higher.

AFM results are compared with PL spectra obtained at 15 K (figures 1–4). The PL full-widths at half-maximum (FWHM) of the samples grown on (100), (110), (311)B and (411)B are 20, 50, 30 and 49 meV, respectively. We observed that the FWHM of the samples that display manganese surface segregation are greater than samples with no segregation on the surface. The increase of PL FWHM is associated with the deterioration of sample quality. These results are further supported by AFM images and XRD spectra as seen in figures 4 and 5, respectively. However, Mn present in the structure is substitutionally incorporated as a result of reduced As defects. Adding very low Mn content into the structure leads to a reduction of As defects and allows the substitutional incorporation of Mn into Ga sites, enabling the observation of optical emission from GaMnAs QW (see figures 1b–4b). Further details can be found in reference [15].

Figure 5 shows the XRD pattern of GaMnAs QW grown at 450°C. Diffraction patterns were obtained with $\theta-2\theta$ from 10 to 90°. The XRD patterns of GaMnAs layers show that the structures are crystallized in the cubic phase. It is well known that the geometry of peaks strongly depends on the positions of the atoms in the crystal [19]. The strongest peaks and grain sizes can be seen for each sample in table 1.

According to the XRD spectra of (100), (110), (311)B and (411)B crystalline planes, 2θ were observed as (31.60–65.86),

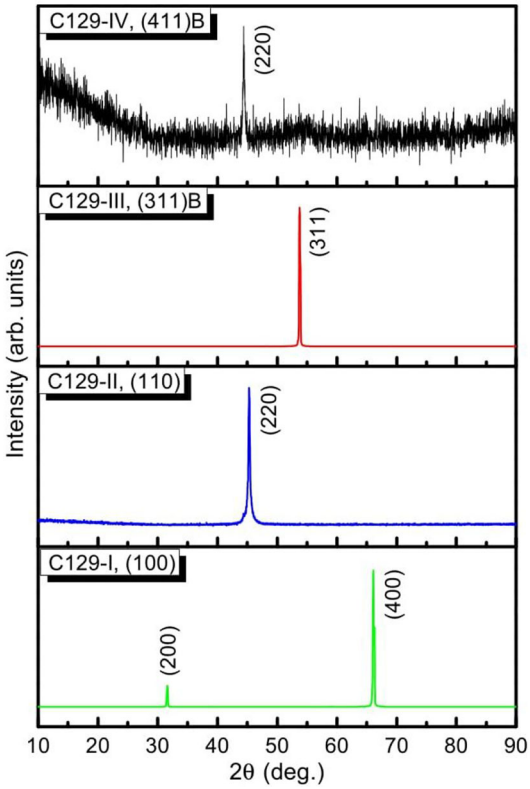

Figure 5. XRD patterns of GaMnAs QW grown on (100), (110), (311)B and (411)B GaAs substrates.

(44.39–66.01), (44.40–53.90) and (44.38–53.44°), respectively. The highest intensity is obtained from the samples grown on (100) and (311)B, in which no Mn segregation occurs on the sample surface. However, the XRD peak intensity is reduced in the samples having Mn segregation on their surface, leading to a degradation of the sample quality. In addition, FWHM of the XRD peaks in (110) and (411)B planes are calculated and found to be much more broader than for (100) and (311)B planes. The FWHM of XRD peaks for (100) and (311)B planes, which do not show any manganese segregation on the surface, are 0.141 and 0.144°, respectively. However, the FWHM of XRD peaks for the samples (110) and (411)B planes are calculated as 0.228 and 0.340°, which are two and three times greater than that of (100) and (311)B, respectively. As a result, the broadness and reduction of XRD peaks intensity might originate from manganese-related defects and manganese segregation. The average grain size (D) was calculated using the Scherrer formula [20].

$$D = \frac{K\lambda}{\beta\cos\theta},$$

where K is a dimensionless shape factor (~0.9), λ (1.5405 Å) is the X-ray wavelength, β is the angular width at the intensity of FWHM and θ is the Bragg angle. The grain size of the samples grown on various orientations showed systematic decrease with increasing manganese segregation on the

Table 1. The standard and calculated X-ray diffraction parameters for $Ga_{0.999}Mn_{0.001}As$.

	Observed data		Standard data				Cell parameters $a = b = c$ (Å)	
Sample	2θ (deg)	d (Å)	2θ (deg)	d (Å)	FWHM (deg)	Grain size (Å)	Calculated	Standard
C129-I	31.55	2.833	31.65	2.825	0.141	610	5.6537	5.6538
	66.10	1.412	66.04	1.414	0.145	682	5.6537	5.6538
C129-II	45.26	2.002	45.35	1.998	0.228	393	5.6537	5.6538
C129-III	53.80	1.703	53.73	1.705	0.144	646	5.6537	5.6538
C129-IV	44.38	2.039	45.35	1.998	0.340	264	5.6537	5.6538

surface as seen in table 1. In accordance with AFM results, the average grain size is found to be 264 and 393 Å for (411)B and (110), respectively. This tends to increase up to 682 and 646 Å in the (100) and (311)B samples, which do not show any segregation, respectively. One can conclude that the grain size is decreased and the FWHM is increased in the samples that have surface manganese segregation. The result is further confirmed by AFM and PL experiments. This might be attributed to manganese-related defects that degrade the surface morphology, and hence the crystal quality, but do not quench the optical emission.

4. Conclusions

We have studied the properties of $Ga_{0.999}Mn_{0.001}As$–AlAs QWs grown on semi-insulating GaAs substrates with various orientations. AFM measurements indicate that Mn distribution is nearly homogenous for the samples grown on (100) and high index (311)B plane across the surface while the (110) and (411)B planes show clear segregation on the surface. XRDs show that samples grown on (100) and (311)B present better crystalline quality than those grown on (110) and (411)B planes. The structural disorder, which causes low crystal quality, is evidenced by XRD results. These results are supported by PL measurements: The samples having no segregation show better optical quality in terms of high intensity of PL signal and low FWHM of the spectra at temperature $T = 15$ K.

Acknowledgements

This work was supported by Adana Science and Technology University [Project Number MÜHDBF.MLZM.2014-13] and The Scientific and Technology Research Council of Turkey (TUBITAK) [Project Number 114F294]. We also acknowledge Brazilian Agencies FAPESP Grant 2012/24055-6 for financial support.

References

[1] Liu Q, Derksen S, Linder A, Scheffer F, Prost W and Tegude F J 1995 *J. Appl. Phys.* **77** 1154
[2] Yang C, Lee S, Shin K W, Oh S, Park J, Kim C Z *et al* 2011 *Appl. Phys. Lett.* **99** 091904
[3] Ohya S, Hai P N, Mizuno Y and Tanaka M 2007 *Phys. Rev. B* **75** 155328
[4] Liu X, Furdyna J K, Dobrowolska M, Lim W L, Xie C and Cho Y J 2007 *J. Phys. Condens. Matter* **19** 165205
[5] Xu J F, Thibado P M, Awo-Affouda C, Ramos F and LaBella V P 2007 *J. Vac. Sci. Technol. B* **25** 1476
[6] Zhao L X, Campion R P, Fewster P F, Martin R W, Ber B Y, Kovarsky A P *et al* 2005 *Semicond. Sci. Technol.* **20** 369
[7] Shimizu H, Hayashi T, Nishinaga T and Tanaka M 1999 *Appl. Phys. Lett.* **74** 398
[8] Yu K M, Walukiewicz W, Wojtowicz T, Lim W L, Liu X, Bindley U *et al* 2003 *Phys. Rev. B* **68** 041308(R)
[9] Johnston-Halperin E, Schuller J A, Gallinat C S, Kreutz T C, Myers R C, Kawakami R K *et al* 2003 *Phys. Rev. B* **68** 165328
[10] Moriya R and Munekata H 2003 *J. Appl. Phys.* **93** 4603
[11] Holy V, Matej Z, Pacherova O, Novak V, Cukr M, Olejnik K *et al* 2006 *Phys. Rev. B* **74** 245205
[12] Dietl T, Ohno H, Matsukura F, Cibert J and Ferrand D 2000 *Science* **287** 1019
[13] Campion R P, Edmonds K W, Zhao L X, Wang K Y, Foxon C T, Gallagher B L *et al* 2003 *J. Cryst. Growth* **251** 311
[14] Nazmul A M, Sugaharaa S and Tanaka M 2003 *J. Cryst. Growth* **251** 303
[15] Gunes M, Erken O, Gumus C, Yalaz E, Pesen E, Ukelge M O *et al* 2016 *Philos. Mag.* **96** 223
[16] Hernández S G, Velis I M, Lopez M R, Kudriats Y, Echavarria A E, Morelhao S L *et al* 2013 *Appl. Phys. Lett.* **103** 192113
[17] Poggio M, Myers R C, Stern N P, Gossard A C and Awschalom D D 2005 *Phys. Rev. B* **72** 235313
[18] Rodrigues D H, Brasil M J S P, Gobato Y G, Holgado D P A, Marques G E and Henini M 2012 *J. Phys. D*: *Appl. Phys.* **45** 215301
[19] Saghrouni H, Missaoui A, Hannachi R and Beji L 2013 *Superlattices Microstruct.* **64** 507
[20] Guneri E, Ulutas C, Kirmizigul F, Altindemir G, Gode F and Gumus C 2010 *Appl. Surf. Sci.* **257** 1189